

Study on the thermal decomposition of capecitabine

Xue-jie Wang¹ · Jin-zong You¹

Received: 17 April 2015 / Accepted: 11 June 2015 / Published online: 3 July 2015
© Akadémiai Kiadó, Budapest, Hungary 2015

Abstract The thermal decomposition of capecitabine (CAP) was measured with thermogravimetry, differential scanning calorimetry, and thermogravimetric analysis coupled with Fourier transform infrared spectroscopy. The IR spectra, high-performance liquid chromatography, and liquid chromatography–mass spectrometry of CAP and the residue of its thermal decomposition at various temperatures were determined. The molecular bond orders were calculated using an ab initio method from the GAMESS program of quantum chemistry. The mode of thermal decomposition for CAP was discussed. The kinetic parameters for thermal decomposition such as activation energy E_a and the pre-exponential factor A were obtained using the Ozawa method. The prospective lifetime of CAP was estimated using the Dakin equation. The results indicated that the thermal decomposition of CAP is a three-step process, and the first mass loss stage is to lose pentyl formate. The initial decomposition temperature in either nitrogen or air is 120 °C. For decomposition in nitrogen, the E_a and A for the initial thermal decomposition are 105.1 kJ mol⁻¹ and 9.12×10^{11} min⁻¹, respectively. For decomposition in air, the corresponding E_a and A are 105.1 kJ mol⁻¹ and 9.55×10^{11} min⁻¹, respectively. The CAP has poor thermal stability under routine temperature.

Keywords Capecitabine (CAP) · Quantum chemistry · Thermal analysis · Mode of thermal decomposition · TG–FTIR · HPLC · LC–MS

Introduction

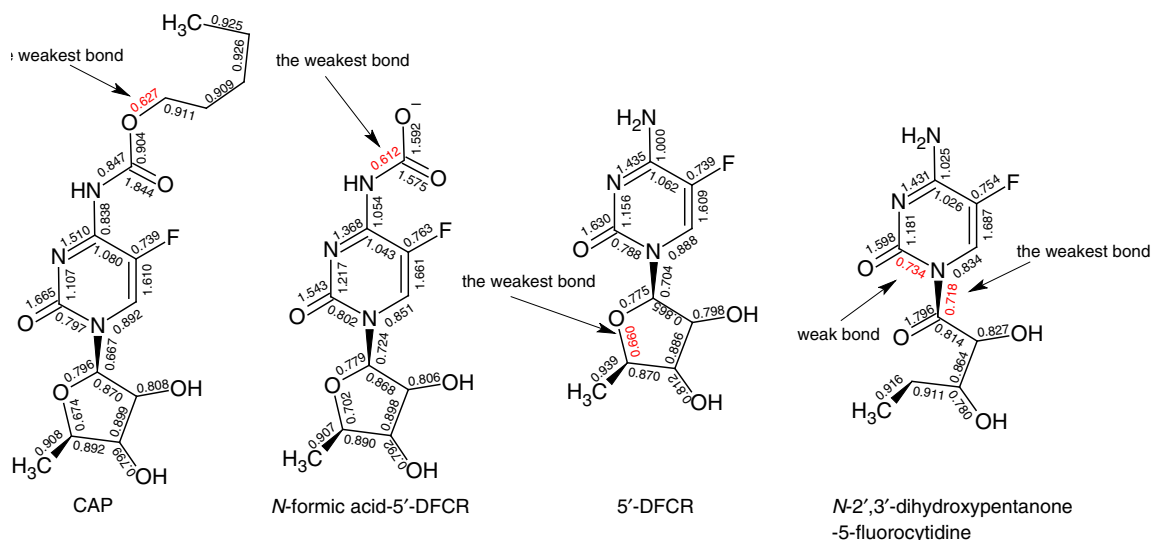
Capecitabine (CAP), with trade name Xeloda, is an orally administered chemotherapeutic agent used in the treatment for numerous cancers [1], such as colorectal cancer [2], breast cancer [3], gastric cancer [4], and esophageal cancer [5]. CAP is a novel 5-fluoropyrimidine carbamate rationally designed as an oral precursor of 5'-deoxy-5-fluorouridine (5'-DFUR). CAP metabolism into 5-fluorouracil (5-FU) requires three sequential enzyme-mediated reaction steps. First, CAP is converted in the liver to 5'-deoxy-5-fluorocytidine (5'-DFCR) by carboxylesterase. The subsequent conversion of 5'-DFCR to 5'-deoxy-5-fluorouridine (5'-DFUR) is mediated by cytidine deaminase, an enzyme found in liver and tumor tissues. Finally, 5'-DFUR is converted to 5-FU by thymidine phosphorylase whose activity is increased in tumor tissue [6]. CAP is composed of three molecular fragments: pentyl formate, 5-fluorocytosine (5-FC) nucleus, and 3,4-dihydroxy-5-methyltetrahydrofuran group. The molecular structure can be seen in Scheme 1.

Thermoanalytical techniques have been widely applied in the pharmaceutical field for several purposes including purity determination for drugs, composition analysis of drugs and raw materials, melting point testing, crystal formation and change tests, thermal stability of medicines, evaluation of the validity, thermal decomposition kinetics, identification of natural drugs, and optimization for production of drugs [7–12].

The results of thermal stability studies and the mode of thermal decomposition of CAP have important theoretical significance for further understanding of the chemical properties of CAP. These considerations may also have practical consequences for the production, processing, and storage of CAP. Although the stability of CAP and its

✉ Xue-jie Wang
xjwang@zisu.edu.cn

¹ School of Science and Technology, Zhejiang International Studies University, Hangzhou 310012, China



Scheme 1 Molecular bond orders of CAP, N-formic acid-5'-DFCR, 5'-DFCR, and N-2',3'-dihydroxypentane-5-fluorocytidine

sustained-release tablets stored at 40 °C in 75 % of relative humidity have been studied [13, 14], the decomposition kinetics of CAP and possible modes of decomposition have not yet been reported. Now, the thermal decomposition processes for CAP in nitrogen and air atmospheres have been examined using thermogravimetric analysis (TG) and differential scanning calorimetry (DSC). The identity of volatile species that evolved during thermogravimetric decomposition was established using Fourier transform infrared spectroscopy (TG-FTIR). Residues of thermal decomposition at different stages were examined using IR spectrometry, high-performance liquid chromatography (HPLC), and liquid chromatography-mass spectrometry (LC-MS). Molecular bond orders for CAP were calculated using an ab initio method from the GAMESS program of quantum chemistry [15, 16]. The kinetics of thermal decomposition of CAP was studied using the Ozawa method [17–19]. The apparent activation energy E_a and pre-exponential factor A for thermal decomposition reactions were obtained from thermogravimetric data under different heating rates. The prospective lifetime of CAP at different temperatures was estimated to provide reference for the correct and reasonable use of this drug.

Experimental

Reagents

The CAP was supplied by Hangzhou Coben Pharmaceutical Co., Ltd. (China). The HPLC purities were 99.5 %. It was used without further purification. 5-FU (99.0 %), 5-FC (99.0 %), 5'-DFCR (98.0 %, i.e., USP Capecitabine

Related Compound A [20]), and 5'-DFUR (98.0 %, i.e., USP Capecitabine Related Compound B [20]) were purchased from the Aladdin Chemistry Co., Ltd. (Shanghai, China). Acetonitrile (ACN) (HPLC purity grade) and ammonium acetate (analytical purity grade) were purchased from Shanghai Zhanyun Chemical Co., Ltd. (Shanghai, China). Ultrapure water was produced by a Millipore Elix3 (Billerica, MA, USA) water purifying system.

Experimental methods

The TG, DTG, and DSC curves for CAP decomposition were obtained using an SDT-Q600 simultaneous thermal analyzer (TA Instruments Inc., USA) and an alumina ceramic crucible containing 8 mg of sample in either nitrogen or air atmospheres (80 mL min⁻¹). The software package provided by the manufacturer was used for estimating the decomposition kinetics and the prospective lifetime for CAP. Four different heating rates were used: 2.0, 5.0, 10.0, 15.0 °C min⁻¹ from ambient to 800 °C.

The residues from thermal decomposition were prepared in an SDT-Q600 simultaneous thermal analyzer using an alumina ceramic crucible containing 10 mg of sample under nitrogen at a flow rate of 80 mL min⁻¹ and heating rate of 10 °C min⁻¹ from room temperature to the selected temperature. Endpoints included the beginning of mass loss, peak of DTG curve, and end of the first mass loss, etc.

The TG-FTIR analysis was conducted using an SDT-Q600 Thermal Analyzer coupled with a Nicolet iS10 FT-IR spectrophotometer (Thermo Fisher Scientific Inc., USA) equipped with a stainless steel transfer line and gas cell. Approximately 20 mg of sample was heated from room

temperature to 700 °C at 20 °C min⁻¹. These experiments were carried out in both dry nitrogen and dry air. The flow rate of gases into the TG–FTIR cell was 80 mL min⁻¹. Both the gas cell for IR detection and the connection line transferring evolved gases from TG to FTIR were kept at 200 °C to prevent gas condensation. The IR spectra of the evolved gases were collected at 6 cm⁻¹ resolution with co-adding of 32 scans per spectrum from 4000 to 500 cm⁻¹.

The IR spectra of CAP and solid residues of thermal decomposition were obtained using a Nicolet iS 10 FT-IR spectrophotometer. The spectra were collected by accumulating 32 scans at a resolution of 4 cm⁻¹ from 4000 to 400 cm⁻¹ using a KBr pellet technique.

Separation studies of standard samples and residues were performed using an HPLC system from Hitachi High-Technologies Corporation of Japan. The instrument consisted of an LC 2130 quaternary gradient pump with a LC 2140 UV–Vis detector. The data were acquired and processed using a HS 2000 chromatography workstation (Hangzhou Science & Technology Co., China). Reversed-phase C-18 columns (250 mm × 4.6 mm i.d. size) containing 5-μm stationary phase were purchased from Shanghai Awence Science & Technology Co., Ltd. The mobile phase consisted of 50 mmol L⁻¹ aqueous ammonium acetate solution as eluent A and ACN as eluent B. Gradient elution started with initial step for 4 min of 2 % B, gradient up to 30 % B in 11 min, then programmed to 40 % B over 5 min, and held for 15 min. The column was purged for 10 min with 2 % B before the next injection. The mobile phase was filtered through a 0.45-μm membrane and degassed via ultrasonication before use. The flow rate was kept constant at 1.0 mL min⁻¹, and the temperature of column was maintained at 35 °C. The 5.0-mg samples (the standard samples or residues from thermal decomposition) were dissolved in 10 mL of mobile phase. A small amount of HAc dilute solution was used to help dissolution. The sample solution was filtered through 0.45-μm membrane before injection. The injection volume was 5 μL and the detection wavelength was 276 nm.

An Agilent 1290 infinity LC system equipped with a G4220A binary pump, G4226A autosampler, and G1330B 1290 thermostat, coupled with a 6460 triple quadrupole mass spectrometer with an electrospray ionization source (Agilent Technologies, USA), was used for LC–MS analysis. The autosampler was maintained at 4 °C, and the column compartment was set at 35 °C. Chromatographic separation was achieved using an Agilent ZORBAX XDB C-18 column (250 mm × 4.6 mm × 5 μm). The mobile phase consisted of ultrapure water as eluent A and ACN as eluent B at a flow rate of 1.0 mL min⁻¹. Gradient elution started with initial step for 4 min of 2 % B, gradient up to 30 % B over 11 min, then programmed to 40 % B over 5 min, and held for 15 min. The column was purged for

10 min with 2 % B before the next injection. The mobile phase was filtered through a 0.45-μm membrane and degassed via ultrasonication before use. The mass spectrometer was operated in both negative and positive ion modes using ESI under the following general conditions: capillary voltage, 3.0 kV (+) or 3.5 kV (–); nozzle voltage, 0 (+) or 500 (–); fragment voltage, 135 V; nebulization pressure, 45 psi; temperature of drying gas, 325 °C; drying gas flow, 5 L min⁻¹; sheath gas temperature, 350 °C; sheath gas flow, 11 L min⁻¹. Data were acquired using the Mass Hunter software (Agilent Technologies, USA) in the multiple reaction monitoring (MRM) mode by recording ion currents for the following transitions: 100–500 m/z. About 10 mg of sample (residue from thermal decomposition) was dissolved in 5 mL of mobile phase. The sample solution was filtered through a 0.45-μm membrane before injection. The injection volume was 10 μL.

Quantum chemical methods

ChemDraw software attached to ChemOffice (Version: Ultra 11.0.1, CambridgeSoft, 2007) was used to predict the molecular structure of CAP. The GAMESS package is a general ab initio quantum chemistry package attached to ChemDraw and was used to calculate molecular energy, charge distribution, and bond order. The HF/6-31G level was used. The calculation accuracy and convergence threshold were the default values in all programs. All the calculations were completed using a personal computer.

Results and discussions

The thermal decomposition process for CAP

The thermal decomposition curves for CAP in nitrogen and air atmospheres obtained at a heating rate of 10 °C min⁻¹ are shown in Fig. 1. It can be seen that the thermal decomposition of CAP occurs in three stages with decomposition beginning at 120 °C. The boundary lines between these three degradations are indistinct, especially the second and third stages. In nitrogen, the first mass loss occurs from 120 to 163 °C, the DTG peak temperature is 143 °C, and the mass loss is 23.7 %. The second mass loss occurs from 163 to 294 °C, the DTG peak temperature is 249 °C, and the mass loss is 30.2 %. From the DTG curves, it can be seen that the second mass loss actually includes a two-step reaction. Over 294 °C is the third mass loss stage, this is a slow mass loss process, and there is about 20 % remnant at 800 °C. In air, first mass loss occurs from 120 to 163 °C, the DTG peak temperature is 143 °C, and the mass loss is 23.9 %. The second mass loss occurs from 163 to

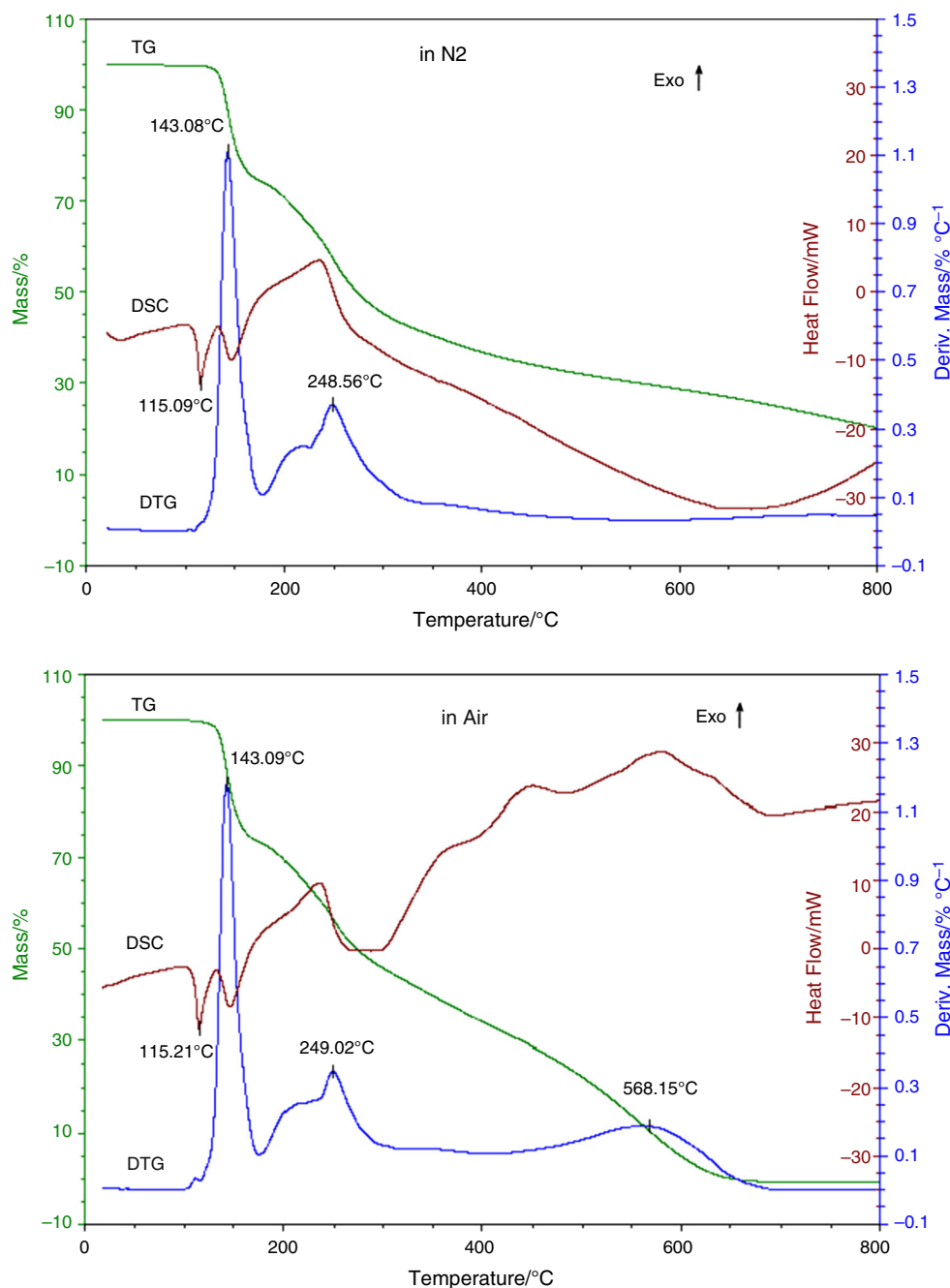


Fig. 1 Thermal analysis curves for CAP (heating rate: $10\text{ }^{\circ}\text{C min}^{-1}$)

$294\text{ }^{\circ}\text{C}$, the DTG peak temperature is $249\text{ }^{\circ}\text{C}$, and the mass loss is 29.6% . The third mass loss occurs from 292 to $670\text{ }^{\circ}\text{C}$, the DTG peak temperature is $568\text{ }^{\circ}\text{C}$, the mass loss is 46.5% , and the decomposition completes about $670\text{ }^{\circ}\text{C}$.

Before the CAP began to lose mass, the DSC curves both have an obvious endothermic peak. This suggests that CAP melts before pyrolysis. In nitrogen, the DSC peak temperature is $115\text{ }^{\circ}\text{C}$ and the melting heat (peak area) is 57.1 J g^{-1} . In air, the DSC peak temperature is $115\text{ }^{\circ}\text{C}$ and the melting

heat of CAP is 58.8 J g^{-1} . The DSC curves corresponding to the first mass loss steps both have an endothermic peak. This suggests that the first stages of thermal decomposition both are a thermal cracking process. The DSC curves corresponding to the second mass loss steps both have an exothermic peak. This suggests that the second mass loss step contains intramolecular or intermolecular oxidation reaction processes. The DSC curve of the third stage in nitrogen is an endothermic peak, which means that this is a

thermal cracking process. The DSC curve of the third stage in air is an exothermic peak, which means that this is an oxidation decomposition process. The thermal analysis curves of the first and the second stages in two atmospheres are almost exactly the same, which means that the thermal decomposition processes of these two stages in two atmospheres are the same. The mass loss rates of the first mass loss steps both are slightly larger than the theoretical value of losing the pentyl group (19.76 %), but both are less than the theoretical value of losing the pentyl formate group (32.0 %). The mass loss rates of the second mass loss steps both are slightly smaller than the theoretical value of losing the 3,4-dihydroxy-5-methyltetrahydro furan ring (32.56 %). This means that these two decomposition stages both are partially synchronous or contain other reactions.

By comparing the thermogravimetric curves at different heating rates, experimental results show that with the increase in heating rate, thermogravimetric curves and the peak temperature of DTG curve T_{\max} move slightly to higher temperature, and the temperature range of every stage and the mass loss rate are slightly decreased. The relationships between heating rate β and DTG peak temperature $T_{\max 1}$ of CAP in nitrogen atmosphere and in air atmosphere are shown in Table 1.

The FTIR analysis of the gaseous species and the solid residues produced by the thermal degradation of CAP [21, 22]

The analysis of the gases produced during the decomposition process can provide valuable information about the pathway of decomposition. TG–FTIR is widely used to analyze the gaseous products during the thermal decomposition [12, 23, 24]. The three-dimensional diagrams of infrared absorption of evolved gas products versus time and wavenumber during the thermal decomposition processes are shown in Fig. 2. The Gram–Schmidt (GS) curves of the TG–FTIR are shown in Fig. 3. TG–FTIR spectra of the gaseous products at different temperatures of the thermal decomposition of CAP are shown in Fig. 4. In contrast to Fig. 1, it can be seen that the GS plots both are similar to the DTG curves, and each GS peaks corresponding to DTG peaks. From Figs. 3 and 4, it can be seen that the IR spectra of the major gaseous products at the *a* point, namely initial stage of thermal decomposition, both contain CH bands (2939 and 2888 cm^{-1}) of alkane. It implies that the initial steps of thermal decomposition both are the fracture of

C–O bond of pentyl formate. The IR spectra of the major gaseous products at the *b* point, namely near the first DTG peak of thermal decomposition, both contain CH bands (2939, 2888, and 1460 cm^{-1}), CO_2 bands (2359 cm^{-1}), H_2O bands (multiplet bands at 3700 m^{-1}), and C–OH band (1047 cm^{-1}). It means that the first stages of thermal decomposition both mainly are the decomposition of pentyl formate. The IR spectra of the major gaseous products at the *c* point, namely near the second DTG peak of thermal decomposition, both contain CH bands, CO_2 band, C–OH band, C=O band (1768 cm^{-1}), and H_2O bands. It means that the second stages of thermal decomposition in two atmospheres both mainly are the decomposition of 3,4-dihydroxy-5-methyltetrahydrofuran ring. The IR spectra of the major gaseous products at the *d* and *e* points in nitrogen atmosphere, namely the bottom of the second stage and the third stage of thermal decomposition, both contain small amount of CO_2 and CO bands. It means that the late second stage and the third stage of thermal decomposition are mainly thermal cracking and small amount of intermolecular and intramolecular oxidation of residues. The IR spectra of the gaseous products at the *d* and *e* points in air atmosphere, namely the bottom of the second stage and the third stage of thermal decomposition, contain large amount of CO_2 and H_2O bands. It means that the late second stage and the third stage of thermal decomposition in air atmosphere are the oxidation decomposition of residues.

The analysis of solid residues formed at various temperatures can also provide direct information on changes that occur in the chemical composition of organic samples during thermal degradation. The infrared spectra of CAP, 5'-DFCR and residues that formed at the various temperature stages during the thermal decomposition processes in nitrogen atmosphere are shown in Fig. 5. From Fig. 5, it can be seen that the IR spectrum of residue obtained at the initial stage of thermal decomposition (130 °C) is similar to that of CAP, but the CH bands (3000–2800 cm^{-1}) are decreased obviously and the C=O band (1760 cm^{-1}) of pentyl formate and the C–O band (1208 cm^{-1}) of ester are decreased. It indicates that the initial step of thermal decomposition is to lose the pentyl formate group. The new presented C=O band (1800 cm^{-1}) means that there is a molecular rearrangement and part of ester changes its structure (acid anhydride or internal ester) during this stage. The IR spectrum of residue formed at the bottom of the first mass loss step (160 °C) shows that the C=O band of formic ester disappears and the C–O band of ester is decreased obviously. It means that the pentyl formate group has lost. Although there is no significant change in the C–OH band (1048 cm^{-1}) and the C–O–C band (1087 cm^{-1}) of glucoside, the IR spectrum of the residue is obviously different from that of 5'-DFCR (the product of CAP losing pentyl formate). It indicates that the residue is mixture and contains nucleoside analogues, and there are

Table 1 Relationship between heating rate β and peak temp. $T_{\max 1}$ of DTG

Atmosphere	Relationship	R^2
In N_2	$T_{\max 1} = 3.921\beta - 0.126\beta^2 + 117.04$	0.993
In air	$T_{\max 1} = 3.705\beta - 0.114\beta^2 + 117.43$	1.0

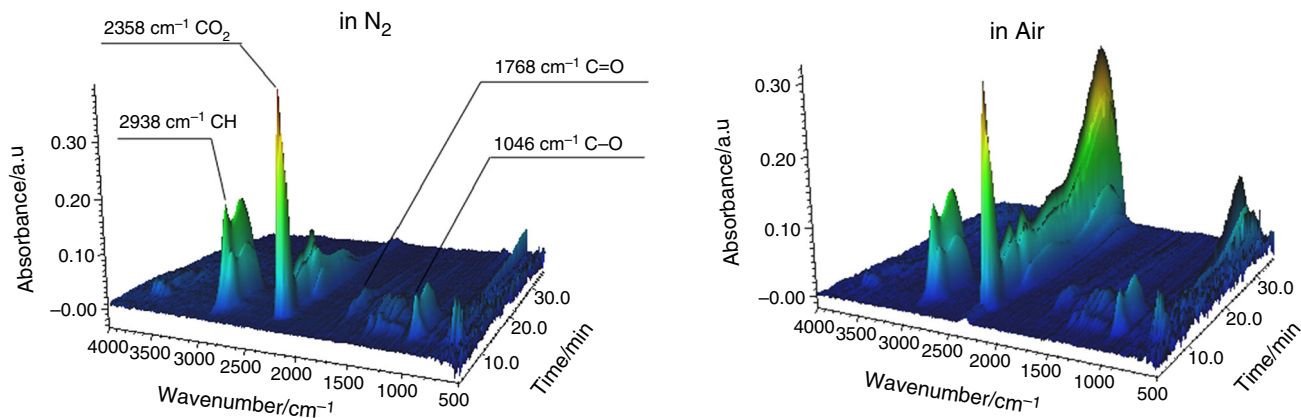


Fig. 2 3D TG-FTIR spectra of the evolved gaseous products of CAP

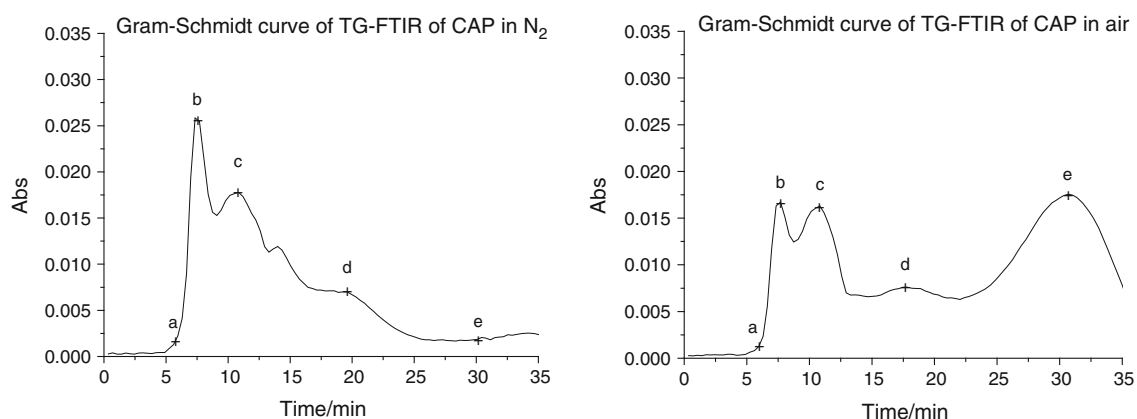


Fig. 3 Gram-Schmidt (GS) curves of the TG-FTIR of CAP

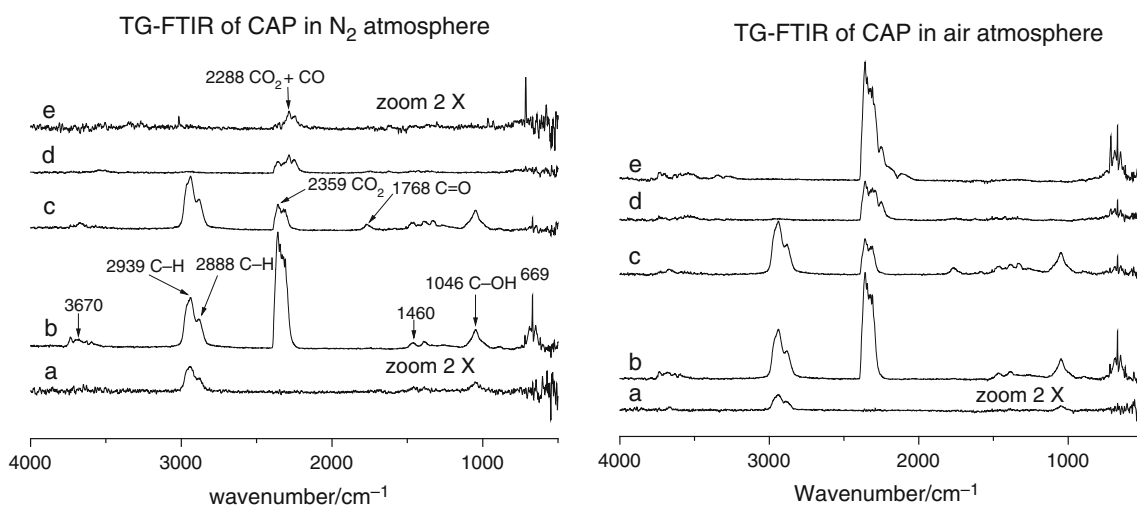


Fig. 4 TG-FTIR spectra of the evolved gaseous products of CAP obtained at different temperatures (*a*, *b*, *c*, *d*, and *e* corresponding to Fig. 3)

other reactions besides losing of pentyl formate at the first mass loss stage. From the IR spectrum of residue formed at the upside of the second stage (210 °C) and the IR

spectrum of residue formed at the middle of the second stage (240 °C), it can be seen that the outline of spectra and the positions of major bands all are similar with the IR

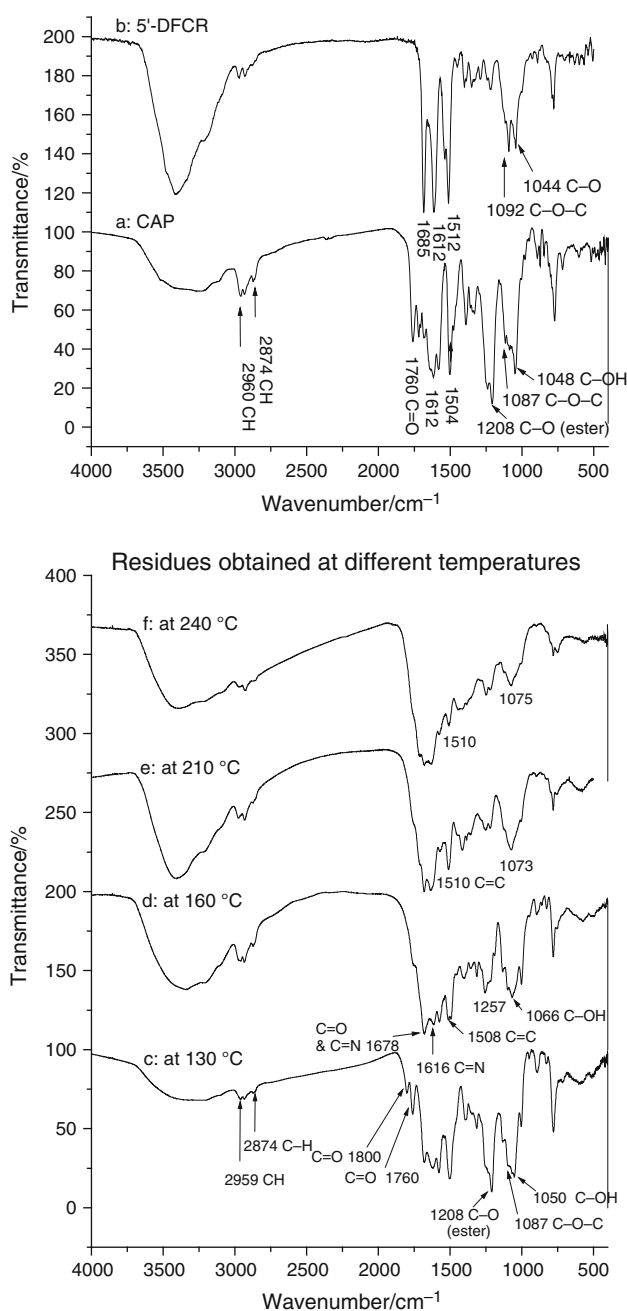


Fig. 5 IR spectra of CAP, 5'-DFCR, and residues of CAP formed at the various temperatures. *a* IR spectrum of CAP; *b* IR spectrum of 5'-DFCR; *c* IR spectrum of residue obtained at 130 °C; *d* IR spectrum of residue obtained at 160 °C; *e* IR spectrum of residue obtained at 210 °C; and *f* IR spectrum of residue obtained at 240 °C

spectrum of residue formed at 160 °C, and there are C=O band (1678 cm^{-1}) and C=N band (1634 cm^{-1}) of 5-FC ring. But these spectra are obviously different from those of 5-FC (the product of 5'-DFCR losing furan ring). It means that the second stage of thermal decomposition just goes through 5-FC stage partially.

HPLC analysis on intermediate residues from the thermal decomposition of CAP

In order to know whether the thermal decomposition of CAP goes through 5'-DFCR and 5-FC stages, the intermediate residues from thermal decomposition were analyzed with HPLC and compared with the chromatograms of standard samples. The results are shown in Fig. 6. The standard samples of 5-FC, 5-FU, 5'-DFCR, 5'-DFUR, and CAP are dissolved in mobile phase and turn into a colorless solution, and their retention times are 3.85, 4.54, 13.71, 14.50, and 21.91 min, respectively. The residue obtained at 130 °C is a canary yellow solid that can be completely dissolved in mobile phase and turn into a colorless solution. Its HPLC chromatogram contains a big peak of 5'-DFCR, three medium peaks of CAP, unknown products X (15.5 min) and Y (24.5 min), and some small peaks including the peak of 5'-DFUR (14.5 min). It means that most of CAP loses pentyl formate to form 5'-DFCR, and part of CAP goes through molecular rearrangement to form unknown products X and Y. Because these rearrangement products remain in residues, the mass loss rates of the first steps are actually less than the theoretical value of losing the pentyl formate group (32.0 %). The 5'-DFUR peak implies that a small number of 5'-DFCR are oxidized to form 5'-DFUR during the first stage of thermal decomposition. The residue of CAP obtained at 160 °C is a brown solid, most of which can be dissolved in mobile phase and turn into a colorless solution, and there is some insoluble

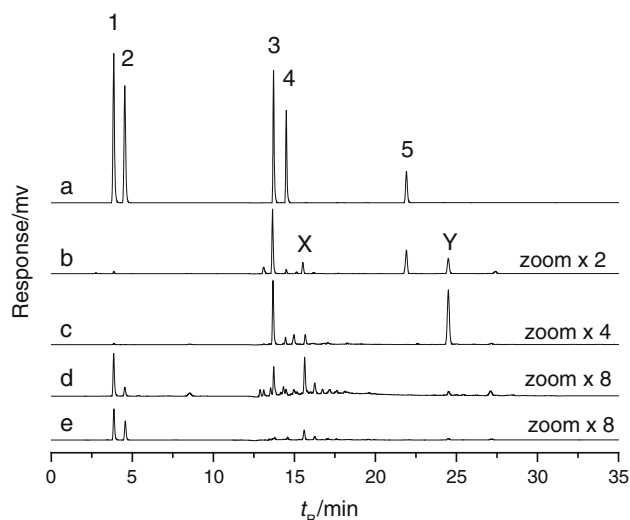


Fig. 6 HPLC chromatograms of residues of CAP in thermal decomposition. *a* Standard samples (every one 0.5 mg mL^{-1}): 1 5-FC, 2 5-FU, 3 5'-DFCR, 4 5'-DFUR, 5 CAP. *b* Residue of CAP formed at 130 °C. *c* Residue of CAP formed at 160 °C. *d* Residue of CAP formed at 210 °C. *e* Residue of CAP formed at 240 °C

precipitate. Its HPLC chromatogram contains a small peak of 5'-DFCR, a small peak of unknown product Y, and some smaller peaks including the peaks of 5'-DFUR (14.5 min) and unknown product X. It means that most of CAP has been decomposed at this temperature. These small peaks and insoluble precipitate imply that part of 5'-DFCR decomposes and carbonizes directly to form insoluble substance and small molecules. The residue of CAP obtained at 210 °C is a black solid, part of which can be dissolved in mobile phase and turn into a colorless solution, and there is much black insoluble precipitate. Its HPLC chromatogram contains very small peaks of 5-FC, 5-FU, 5'-DFCR, 5'-DFUR, unknown product X, and other unknown products. These very small peaks and insoluble precipitate indicate that most of 5'-DFCR decomposes and carbonizes directly to form black insoluble substance and small molecules. The small peak of 5-FC implies that part of 5'-DFCR loss 3,4-dihydroxy-5-methyltetrahydrofuran ring to form 5-FC during the second decomposition stage. The 5-FU and 5'-DFUR peaks indicate that intermolecular or intramolecular oxidation reactions occur during the decomposition, some of 5'-DFCR is oxidized to 5'-DFUR, some of 5-FC is oxidized to 5-FU, and some of 5'-DFUR decomposes to 5-FU. The residue of CAP obtained at 240 °C is a black spumescent solid, trace of which can be dissolved in mobile phase and turn into a colorless solution, and there is much black insoluble precipitate. Its HPLC chromatogram contains very small peaks of 5-FC, 5-FU, and other unknown products. It means that most of 5'-DFCR has been decomposed at this temperature.

LC-MS analysis on intermediate residues from the thermal decomposition

In order to confirm the composition of the residue, the soluble fraction of the residues formed at 130 and 240 °C were analyzed using LC-MS method, and the results are shown in Figs. 7 and 8, respectively. The LC-MS analysis of residue formed at 130 °C indicates that the HPLC peaks of I, II, and IV in Fig. 7 are 5'-DFCR, 5'-DFUR, and CAP, respectively. The molecular weights of III and V, namely unknown products X and Y, are 386 and 341, respectively. The molecular weight of X is larger than that of CAP (359), and the retention time of X is less than that of CAP. It means that the polarity of X is larger than that of CAP. The molecular weight of Y is less than that of CAP, and the retention time of Y is greater than that of CAP. It means that the polarity of Y is less than that of CAP. These indicate that the unknown product X and Y are molecular rearrangement products (the structures have not been confirmed). The LC-MS analysis of residue formed at 240 °C indicates that the HPLC peaks of VI and VII in

Fig. 8 are 5-FC and 5-FU, respectively. The results of LC-MS confirm the results of HPLC.

Thermal decomposition mode of CAP

Theoretically, the thermal decomposition of organic molecules is due to the molecular kinetic energy increasing during heating. These include atomic oscillations that rupture the weaker chemical bonds. Lower chemical bond order offers easier fracture. Thermodynamically, the decomposition process also depends on the stability of the decomposition products or intermediates generated. In order to understand the pyrolysis mode of CAP, a theoretical discussion is made from the perspective of the molecular structure. A quantum chemical ab initio method is used to calculate molecular charge distribution and the bond orders for CAP and intermediates (Scheme 1). According to the molecular bond order distributions of CAP and intermediates, the position and sequence of the chemical bonds ruptured could be judged, and the pyrolysis mode of CAP in the pyrolysis process could be speculated. From Scheme 1, it can be seen that the weakest bond of CAP is the C-O bond (0.627) of pentyl formate. It will rupture first and lose pentyl group and to form unstable intermediate N-formic acid-5'-DFCR. The weakest bond of N-formic acid-5'-DFCR intermediate is the C-N bond (0.612) of N-formate acid. It will follow closely to rupture and to form a relatively stable 5'-DFCR. So, the losing pentyl formate is the main reaction process of the first mass loss steps during the thermal decomposition. The weakest bond of 5'-DFCR is the C-O bond (0.660) in furan ring. It will rupture to form unstable intermediate *N*-2',3'-dihydroxypentanone-5-fluorocytidine with increasing temperature. The weakest bond of *N*-2',3'-dihydroxypentanone-5-fluorocytidine is the *N*-glycosidic bond (0.718) that connects the 5-FC ring and the furan ring, and the second weak bond is C-N bond (0.734) of amide in 5-FC ring. These two bond orders are so close that they will rupture at about the same time. The rupture of the *N*-glycosidic bond leads to 5-FC, and the rupture of amide C-N bond leads to complete decomposition of *N*-2',3'-dihydroxypentanone-5-fluorocytidine. So, there is part of 5'-DFCR that directly decomposes to insoluble substance, and part of 5'-DFCR decomposes to 5-FC in the second mass loss stage.

The amino group at 5-FC ring is easy to be oxidated, the C-O bonds in furan ring are weak and easy to break, and some free oxygen is formed during the decomposition of the furan ring. The free oxygen will oxidize amino to hydroxyl or carboxide. So, some oxidation products can be found in the residues. The thermal decomposition processes of CAP contain intramolecular oxidation reaction at the second stage. Therefore, the DSC curve of the second stage shows as an exothermic peak.

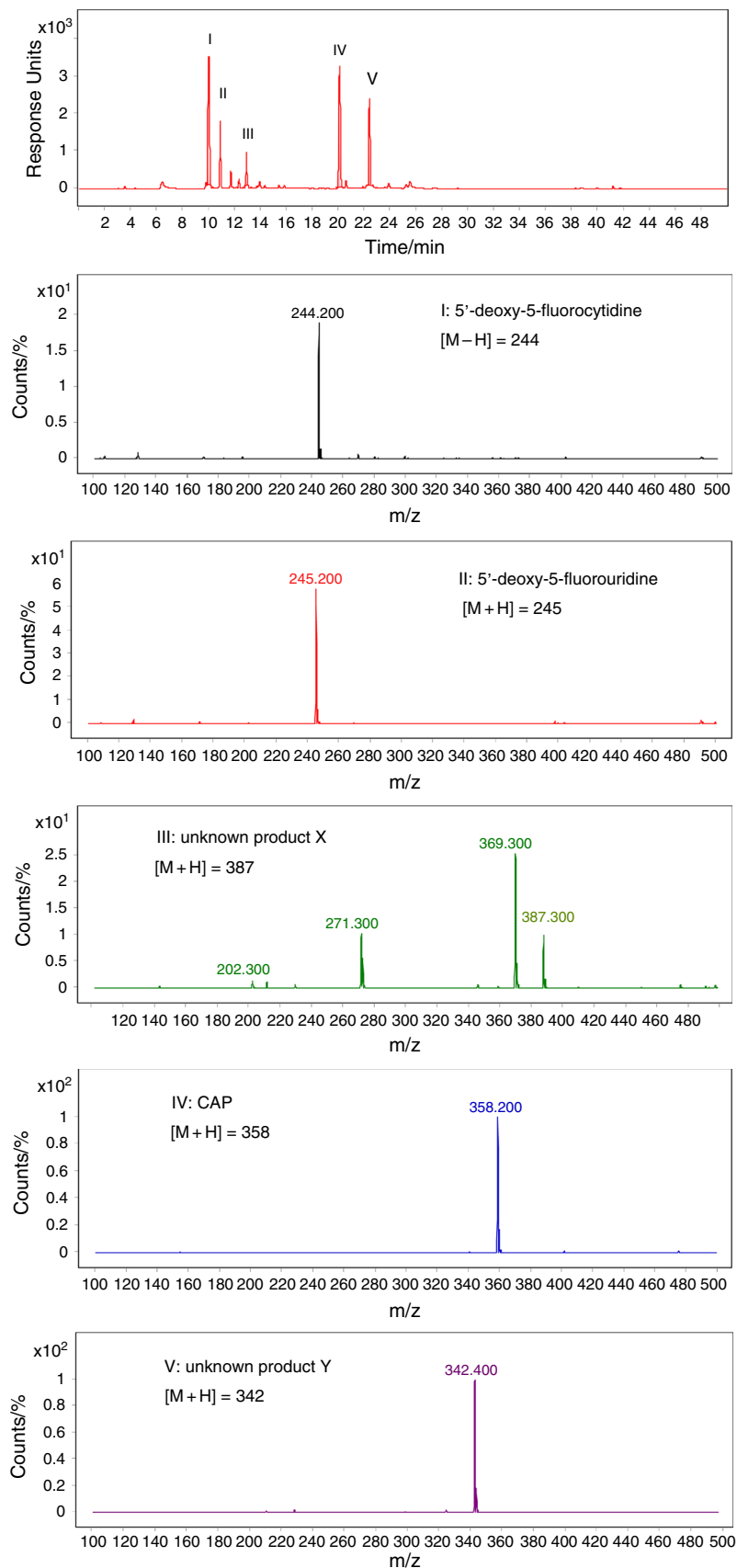
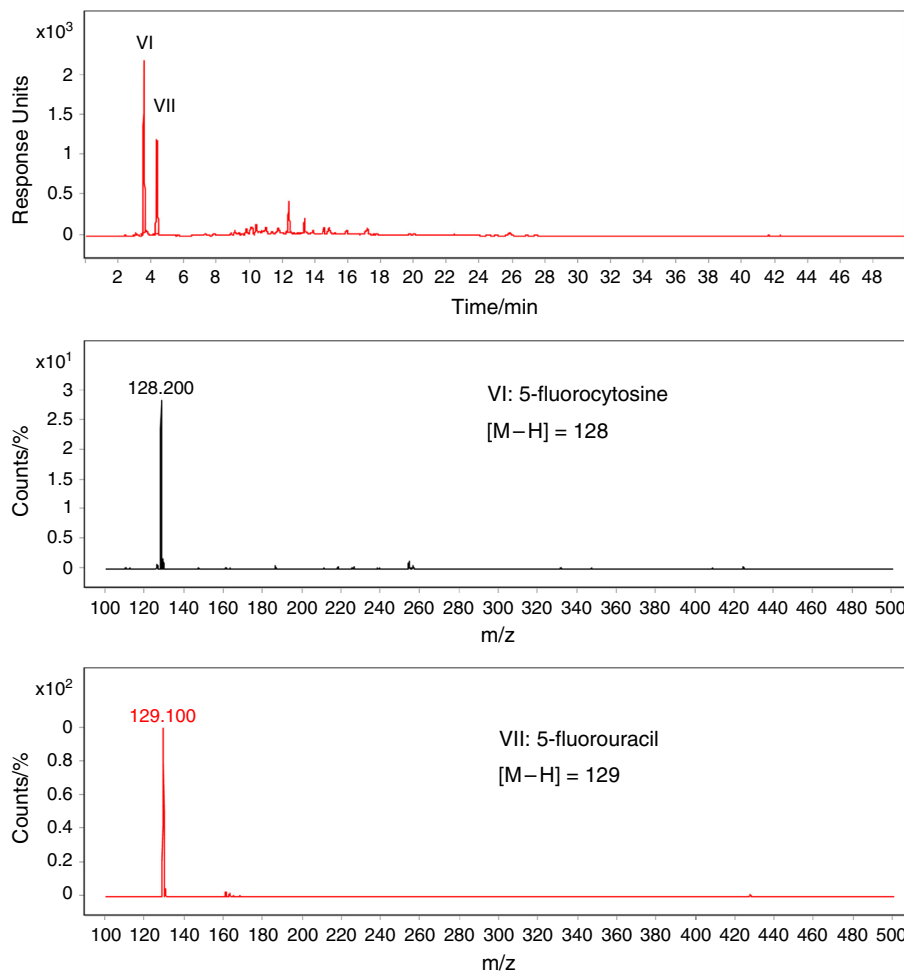
Fig. 7 LC-MS results of CAP residue obtained at 130 °C

Fig. 8 LC–MS results of CAP residue obtained at 240 °C



After comprehensive analysis of the above, speculated mode of thermal decomposition process for CAP is shown in Scheme 2.

Kinetics of thermal degradation of CAP in nitrogen and in air atmosphere

The thermal decomposition kinetics of CAP was studied using the ASTM E 1641 method [17]. This method is also known as the multiple heating rate method or the equal conversion rate method. This method does not use the model function of thermal decomposition. The activation energy E_a and pre-exponential factor A are calculated independently based on the data that are determined from the same conversion rate of TA curves under different heating rate. Therefore, this method is also known as the model-free method.

The basic principle of this method is that the thermal decomposition reaction rate constant k relates to temperature T via the Arrhenius equation:

$$k = A \exp(-E_a/RT) \quad (1)$$

where k is reaction rate constant, t^{-1} ; A is the pre-exponential factor, min^{-1} ; E_a is the activation energy, J mol^{-1} ; R is the gas constant, $8.314 \text{ J K}^{-1} \text{ mol}^{-1}$; and T is the absolute temperature in Kelvin.

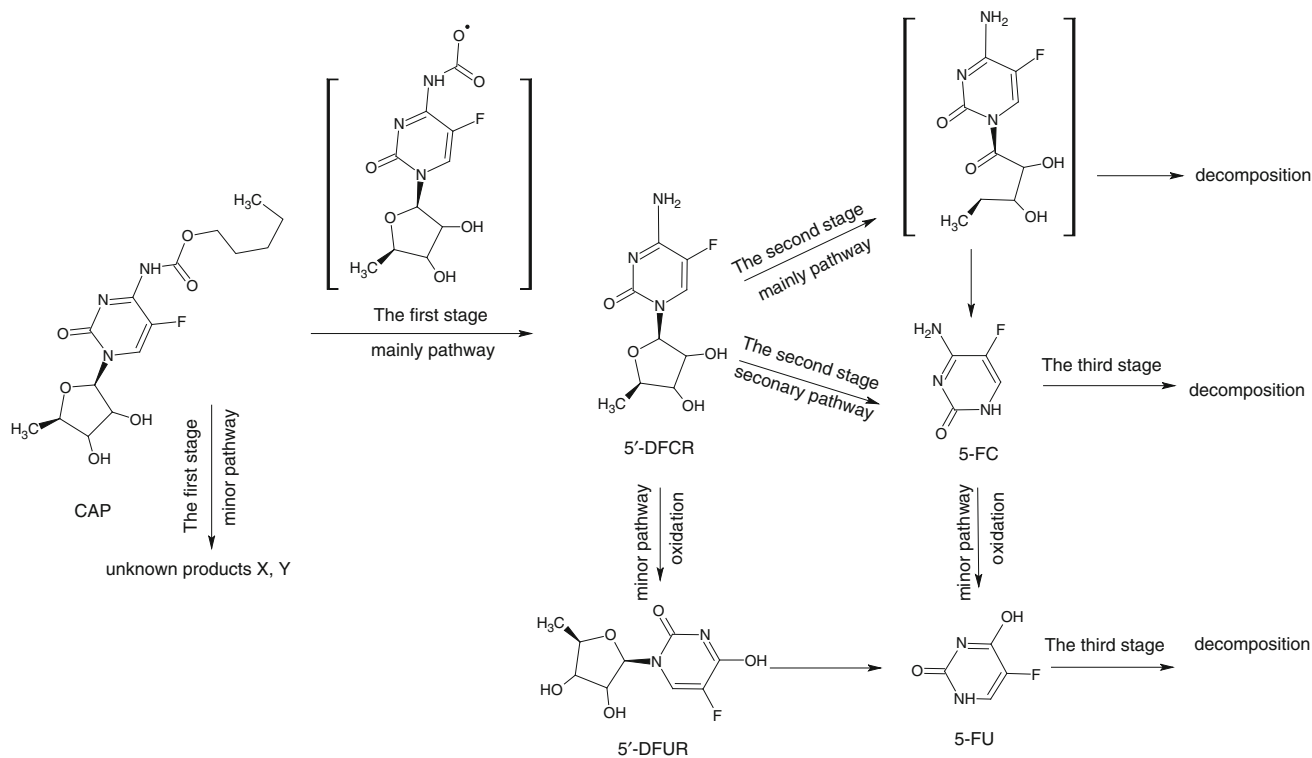
Ozawa [18], Flynn and Wall [19] deduced a thermodynamic approximate relationship between the heating rate β and the corresponding temperature T at a given conversion:

$$\lg \beta + 0.4567(E_a/RT) = \text{constant} \quad (2)$$

To convert α_1 using heating rates β_1 , β_2 , and β_3 , with corresponding temperatures T_1 , T_2 , and T_3 , Eq. (3) was obtained.

$$\begin{aligned} \lg \beta_1 + 0.4567(E_a/RT_1) &= \lg \beta_2 + 0.4567(E_a/RT_2) \\ &= \lg \beta_3 + 0.4567(E_a/RT_3) \end{aligned} \quad (3)$$

The Arrhenius activation energy is then determined from a plot of the logarithm of heating rate versus the reciprocal of the absolute temperature at a constant conversion level. The same linear relationship exists for the different conversions α_2 , α_3 , and α_4 . Then, the pre-exponential factor A can be obtained from Eq. (4).



Scheme 2 Postulated mode of thermal decomposition for CAP

$$A = \beta(E_a/RT) \exp(E_a/RT) \quad (4)$$

The experimental data were processed with Eqs. (3) and (4). The kinetic activation energy E_a and pre-exponential factor A under different conversion rates at each stage of thermal decomposition process could be obtained. The calculated kinetic parameters of the first and second stages for the CAP are listed in Table 2, and the kinetic rate constants of thermal decomposition for CAP at the initial

stages are expressed as Eqs. (5) and (6). The kinetic parameters of the third stage cannot be obtained because the decomposition rate is very slow.

$$\text{in } N_2 \quad k_1 = 9.12 \times 10^{11} \exp(-105.1 \times 10^3/RT) \quad (5)$$

$$\text{in air} \quad k_1 = 9.55 \times 10^{11} \exp(-105.1 \times 10^3/RT) \quad (6)$$

The decomposition of CAP in two atmospheres is a three-step process. From Table 2, it can be seen that at the

Table 2 Kinetic parameters of CAP at the 1st and 2nd stages

Stage	Mass loss $\alpha/\%$	In N_2		In air	
		Activation energy $E_a/\text{kJ mol}^{-1}$	pre-exponential factor A $\text{Log}/A \text{ min}^{-1}$	Activation energy $E_a/\text{kJ mol}^{-1}$	pre-exponential factor A $\text{Log}/A \text{ min}^{-1}$
The first stage	5.0	105.1	11.96	105.1	11.98
	10.0	104.7	12.06	104.5	12.16
	15.0	101.6	11.69	104.5	12.10
	20.0	116.4	13.52	106.7	12.33
The second stage	25.0	124.1	14.14	120.6	13.74
	30.0	124.7	13.17	121.2	12.79
	35.0	137.4	14.03	132.8	13.54
	40.0	160.2	15.92	152.4	15.11
	45.0	191.8	18.71	200.8	19.59
	50.0	289.1	27.68	390.0	37.23

Table 3 Prospective lifetime of CAP at different usage temperatures

Temperature/°C	In N ₂		In air	
	Rate constant/min ⁻¹	Lifetime/h	Rate constant/min ⁻¹	Lifetime/h
25	3.471×10^{-7}	2.59×10^3	3.643×10^{-7}	2.54×10^3
125	1.470×10^{-2}	6.11×10^{-2}	1.539×10^{-2}	6.02×10^{-2}
225	8.636	1.04×10^{-4}	9.037	1.03×10^{-4}
325	6.020×10^2	1.49×10^{-6}	6.295×10^2	1.47×10^{-6}
425	1.244×10^4	7.22×10^{-8}	1.300×10^4	7.13×10^{-8}

beginning of decomposition, about 20 % mass loss is the first stage, mass loss of 25 % to 50 % is the second stage, and from 50 % to complete decomposition is the third stage. There are conversion ranges between each two stage, in which the kinetic parameters change obviously. The different activation energy E_a and pre-exponential factor A indicate that the decomposition mode of the two stages is different. The change of the kinetic parameters in the first stage is small, which indicates that the first stage is a simple pyrolysis reaction. The change of the kinetic parameters in the second stage is large, which indicates that the second stage is a complex reaction. The kinetic parameters of the initial stage in two atmospheres are nearly the same. So, the decomposition temperature and decomposition rate of CAP in two atmospheres are nearly the same.

Dakin [25] showed that the lifetime of the material (at a given conversion) has a linear relationship with the reciprocal of temperature:

$$\lg \tau = a/T + b \quad (7)$$

Here, τ is the prospective lifetime and T is thermodynamics temperature. This equation had also been used to predict the lifetime of medicines [26]. This equation can be derived from the reaction rate equation and is a universal equation. Specifically, $a = E_a/2.303 R$, and b is a constant at a given conversion rate α and corresponds to the pre-exponential factor and the thermal reaction function mode. The temperature and time under the different heating rate at a given conversion rate α are obtained by experiments. A linear relationship is obtained from a plot of the logarithm of time ($\log t$) versus the reciprocal of temperature $1/T$, i.e., the Dakin equation. It can be used to speculate the lifetime of a drug at different temperatures. Using 5 % mass loss as the lifetime of the drug, some calculated prospective lifetimes of CAP are shown in Table 3.

The data in Table 3 indicate that the CAP has poor thermal stability and that it can be preserved for short-term storage under normal temperature and air atmosphere. The temperature should be controlled in the production, drying, and storage to ensure drug quality.

Conclusions

The thermal analysis for CAP shows that the thermal decomposition processes of CAP are three-step processes in both nitrogen and air. There is a melting process before the decomposition. The infrared spectra, HPLC, and LC-MS of CAP and its residues at different temperatures during the pyrolysis processes were determined. The molecular bond orders for CAP and intermediates were calculated using an ab initio quantum chemistry method (GAMESS program), and the thermal decomposition mode of CAP was discussed. The starting thermal decomposition step of CAP is to lose the pentyl formate, and the decomposition process of CAP is a multi-step and multi-path process. The Ozawa method was used to calculate the kinetic parameters of the thermal decomposition reaction of CAP, the apparent activation energy (E_a), and pre-exponential factor (A). The initial decomposition temperature in both nitrogen and air is 120 °C. For decomposition in nitrogen, the activation energy E_a and the pre-exponential factor A for the initial stages are 105.1 kJ mol⁻¹ and 9.12×10^{11} min⁻¹, respectively. For decomposition in air, the corresponding E_a and A are 105.1 kJ mol⁻¹ and 9.55×10^{11} min⁻¹, respectively. The calculation shows that the CAP has a poor thermal stability. It can be preserved for short-term storage under normal temperature and air atmospheres. The temperature should be controlled in the production, drying, and storage to ensure drug quality.

Acknowledgements This study was financially supported by Zhejiang Provincial Government of China (No. 2011C11032) and Zhejiang International Studies University (No. 07029005).

References

- Rossi S, editors. Australian Medicines Handbook (2013 ed.). Adelaide: The Australian Medicines Handbook Unit Trust. 2013.
- Cunningham D, Coleman R. New options for outpatient chemotherapy the role of oral fluoropyrimidines. *Cancer Treat Rev.* 2001;27:211–20.

3. Leonard R, Hennessy BT, Blum JL, O'Shaughnessy J. Dose-adjusting capecitabine minimizes adverse effects while maintaining efficacy: a retrospective review of capecitabine for metastatic breast cancer. *Clin Breast Cancer*. 2011;11(6):349–56.
4. Sharma SP. Capecitabine and irinotecan in advanced gastric cancer. *Lancet Oncol*. 2007;8(7):577.
5. Li B, Yan J, Zhou T, Wang Z, Li H, Sun H. A phase I study of concurrent late course accelerated hyper-fractionated radiotherapy and capecitabine and cisplatin for local advanced esophageal cancer. *Int J Radiat Oncol*. 2008;72(1):S283.
6. Shimma N, Umeda I, Arasaki M, Murasaki C, Masubichi K, Kohchi Y, Miwa M, Ura M, Sawada N, Tahara H, Kuruma I, Horii I, Ishitsuka H. The design and synthesis of a new tumor-selective fluoropyrimidine carbamate, capecitabine. *Bioorg Med Chem*. 2000;8(7):1697–706.
7. Tao YT, Zhan D, Zhang KL. Kinetics of thermal decomposition of racecadotril in air. *Acta Chim Sin*. 2006;64(5):435–8 (in Chinese).
8. Zhang J, Sheng RL, Mai WP. Studies on the thermal decomposition process and kinetics of purine drugs. *Acta Pharm Sin*. 2002;3(7–8):644–8 (in Chinese).
9. Wang XJ, You JZ. Thermal decomposition mechanism and kinetics of stavudine. *Chin J Appl Chem*. 2011;28(6):709–15 (in Chinese).
10. Rompay JV. Purity determination and evaluation of new drug substances. *J Pharm Biomed Anal*. 1986;4:725–32.
11. Giron D, Goldbronn C. Use of DSC and TG for identification and quantification of the dosage form. *J Therm Anal*. 1997;48:473–83.
12. Silva ACM, Gálico DA, Guerra RB, Perpétuo GL, Legendre AO, Rinaldo D, Bannach G. Thermal stability and thermal decomposition of the antihypertensive drug amlodipine besylate. *J Therm Anal Calorim*. 2015;120:889–92.
13. Łaszcz M, Trzcńska K, Filip K, Szyrowska A, Mucha M, Krzeczyński P. Stability studies of capecitabine. *J Therm Anal Calorim*. 2011;105:1015–21.
14. Davoudi ET, Noordin MI, Javar HA, Kadivar A, Ashjari M, Chermahini SH. Stability study of the gastric floating dosage form of capecitabine. *J Therm Anal Calorim*. 2014;115:2495–9.
15. Schmidt MW, Baldrige KK, Boatz JA, Elbert ST, Gordon MS, Jensen JJ, Koseki S, Matsunaga N, Nguyen KA, Su S, Windus TL, Dupuis M, Montgomery JA. General atomic and molecular electronic structure system. *J Comput Chem*. 1993;14:1347–63.
16. Alexeev Y, Mazanetz MP, Ichihara O, Fedorov DG. GAMESS as a free quantum-mechanical platform for drug research. *Curr Top Med Chem*. 2012;12(18):2013–33.
17. American Society for Testing and Materials. ASTM E1641-99. 1999. <http://www.astm.org/DATABASE.CART/HISTORICAL/E1641-99.htm>.
18. Ozawa T. A new method of analyzing thermogravimetric data. *Bull Chem Soc Jpn*. 1965;38:1881–6.
19. Flynn JH, Wall LA. A quick direct method for the determination of activation energy from thermogravimetric data. *J Polym Sci B*. 1966;4:323–8.
20. The United States Pharmacopeial Convention. Capecitabine. The 35th revision of the United States Pharmacopeia/National Formulary (USP 35-NF30). Washington, 2011;2469–71.
21. Xie JX, Chang JB, Wang XM. Applications of infrared spectroscopy in organic chemistry and medicinal chemistry. Beijing: Science Press; 2001 (in Chinese).
22. NIST Chemistry Webbook Standard Reference Database, 2011, 69 release. <http://webbook.nist.gov/chemistry>
23. Fulias A, Vlase G, Grigorie C, Ledet, i I, Albu P, Bilanin M, Vlase T. Thermal behaviour studies of procaine and benzocaine part 1: kinetic analysis of the active substances under non-isothermal conditions. *J Therm Anal Calorim*. 2013;113:265–71.
24. Amorim PHO, Ferreira APG, Machado LCM, Cervini P, Cavaleiro ETG. Investigation on the thermal behavior of b-blockers antihypertensives atenolol and nadolol using TG/DTG, DTA, DSC, and TG–FTIR. *J Therm Anal Calorim*. 2015;120:1035–42.
25. Dakin TW. Electrical insulation deterioration treated as a chemical rate phenomena. *AIEE Trans Part I Commun Electron*. 1948;67:113–22.
26. Zhang LJ, Pang JX, Bai JH. Thermogravimetry study of the lifetime of azithromycin. *J Hebei Normal Univ (Nat Sci Ed)*. 2001;25(4):488–9 (in Chinese).